



**Queensland University of Technology**  
Brisbane Australia

This is the author's version of a work that was submitted/accepted for publication in the following source:

Cejka, Jiri, Sejkora, Jiri, Plasil, Jakub, [Keeffe, Eloise C.](#), [Bahfenne, Silmarilly](#), [Palmer, Sara J.](#), & [Frost, Ray L.](#) (2011) A raman and infrared spectroscopic study of Ca<sup>2+</sup> dominant members of the mixite group from the Czech Republic. *Journal of Raman Spectroscopy*, 42(5), pp. 1154-1159.

This file was downloaded from: <http://eprints.qut.edu.au/41930/>

© Copyright 2010 John Wiley & Sons, Ltd.

**Notice:** *Changes introduced as a result of publishing processes such as copy-editing and formatting may not be reflected in this document. For a definitive version of this work, please refer to the published source:*

<http://dx.doi.org/10.1002/jrs.2817>

1 **Raman microscopy of the mixite mineral  $\text{BiCu}_6(\text{AsO}_4)_3(\text{OH})_6 \cdot 3\text{H}_2\text{O}$  from the Czech**  
2 **Republic.**

3  
4 **Ray L. Frost,<sup>1</sup> • Jiří Čejka,<sup>1,2</sup> Jiří Sejkora,<sup>2</sup> Jakub Plášil,<sup>2</sup> Silmarilly Bahfenne,<sup>1</sup>**  
5 **and Sara J. Palmer<sup>1</sup>**

6  
7 <sup>1</sup> Inorganic Materials Research Program, School of Physical and Chemical Sciences,  
8 Queensland University of Technology, GPO Box 2434, Brisbane Queensland 4001,  
9 Australia.

10  
11 <sup>2</sup> National Museum, Václavské náměstí 68, CZ-115 79 Praha 1, Czech Republic.

12  
13 **ABSTRACT:**

14  
15 **Raman microscopy of the mixite mineral  $\text{BiCu}_6(\text{AsO}_4)_3(\text{OH})_6 \cdot 3\text{H}_2\text{O}$**   
16 **from Jáchymov and from Smrkovec (both Czech Republic) has been**  
17 **used to study their molecular structure, which is interpreted and the**  
18 **presence of  $(\text{AsO}_4)^{3-}$ ,  $(\text{AsO}_3\text{OH})^{2-}$ ,  $(\text{PO}_4)^{3-}$  and  $(\text{PO}_3\text{OH})^{2-}$  units,**  
19 **molecular water and hydroxyl ions were inferred. O-H...O hydrogen**  
20 **bond lengths were calculated from the Raman and infrared spectra**  
21 **using Libowitzky's empirical relation. Small differences in the Raman**  
22 **spectra between both samples were observed and attributed to**  
23 **compositional and hydrogen bonding network differences.**

24  
25 **KEYWORDS:** mixite, arsenate, hydrogen arsenate, phosphate, hydrogen phosphate Raman,  
26 infrared, spectroscopy, molecular water, hydroxyl ions, hydrogen bonds, O-  
27 H...O hydrogen bond lengths  
28

29  
30  
31  
32  
33  
34  

---

\* Author to whom correspondence should be addressed (r.frost@qut.edu.au)

## 35 INTRODUCTION

36

37 Minerals of the mixite group have the general formula  $MCu_6(TO_4)_3(OH)_6 \cdot 3 H_2O$ .  
38 Cations such as  $Ca^{2+}$ ,  $Pb^{2+}$ ,  $Al^{3+}$ ,  $Bi^{3+}$ ,  $Y^{3+}$  and other  $REE^{3+}$  are found to occupy the  
39 octahedrally coordinated M site; only As and P have been found in significant amounts at the  
40 T tetrahedral site. Minerals of this group have been classified on the basis of the occupancy  
41 of the M and T sites: mixite [Bi; As], agardite-(Y) [Y; As], goudeyite [Al; As], petersite-(Y)  
42 [Y; P], zálesíite [Ca; As], agardite-(La) [La; As], agardite-(Ce) [Ce; As], plumboagardite [Pb,  
43 As] and calciopetersite [Ca, P]<sup>1-4</sup>. The names agardite-(Nd), agardite-(Dy) and petersite-(Nd)  
44 were occasionally used<sup>2,5</sup> but these minerals have not been approved by the IMA<sup>4</sup>. Large  
45 extent of isomorphy in the proportion of the major cations and tetrahedral site ( $As \leftrightarrow P$ ), too,  
46 is well documented on the natural members of this group<sup>6-8</sup>. Substitution of a trivalent cation  
47 ( $Bi^{3+}$ ,  $Y^{3+}$ ,  $REE^{3+}$ ) at the M site by divalent ones ( $Ca^{2+}$ ,  $Pb^{2+}$ ) is charge balanced by  
48 concomitant substitution of  $OH^-$  for  $O^{2-}$  at the O(3) site in the crystal structure (attributed to  
49  $AsO_3OH$  group)<sup>1,3,4,9</sup>. The crystal structure of natural members of mixite group reveal  
50 microporous framework<sup>9-10</sup> and some  $H_2O$  groups may well have a zeolitic character<sup>8,11-13</sup>.

51

52 Mixite, hydrated copper bismuth arsenate, with ideal formula  
53  $BiCu_6(AsO_4)_3(OH)_6 \cdot 3H_2O$  was first found in 1880 on the Geister vein at Jáchymov (Czech  
54 Republic) by mine engineer Anton Mixa<sup>14</sup>. It crystallizes in the hexagonal space group  
55  $P6_3/m$ <sup>10</sup> and typically occurs as green radiating acicular prisms and fibrous encrustations.  
56 Mixite, similarly as other minerals of the mixite group, occurs as a supergene mineral in the  
57 oxide zone of ore occurrences and deposits in close association with bismutoferrite,  
58 bismutite, walpurgite and other supergene minerals.

59

60 Infrared and Raman spectra of some minerals of the mixite group and their synthetic  
61 analogues (mixite<sup>15,16</sup>, agardite<sup>17,18</sup>, goudeyite<sup>19</sup>) have been studied. From the published  
62 Raman and infrared spectra, it was inferred that in the structure of these compounds may be  
63 present beside of  $(AsO_4)^{3-}$  also  $(HAsO_4)^{2-}$  and  $(H_2AsO_4)^-$  ions because of necessary charge  
64 balance. However, any presence of the  $(H_2AsO_4)^-$  ion in such structures is very doubtful and  
65 does not agree with the structure analysis.

66

67 This paper is a part of a vibrational spectroscopic investigation on supergene minerals  
68 originating in oxidation zone<sup>20-24</sup>. The aim of this paper is to characterise mixite samples

69 from two Czech occurrences (Jáchymov, Smrkovec) using Raman and infrared spectroscopy,  
70 and to compare the results with their chemical composition. Recently, Raman spectroscopy  
71 has proved to be a most useful tool for the study of molecular structure of minerals containing  
72 oxyanions<sup>25-27</sup>.

73

## 74 **EXPERIMENTAL**

75

### 76 **Minerals**

77 The studied samples of the mineral mixite were found at the Smrkovec ore  
78 occurrence, the Slavkovský les Mountains, western Bohemia, Czech Republic<sup>28</sup>, and at the  
79 Rovnost deposit, the Jáchymov ore district, the Krušné hory Mountains, Northern Bohemia,  
80 Czech Republic. The samples were analysed for phase purity by X-ray powder diffraction  
81 and no minor significant impurities were found. Their refined unit-cell parameters for  
82 hexagonal space group  $P6_3/m$   $a=13.637(1)$ ,  $c=5.910(1)$  Å,  $V=951.8(2)$  Å<sup>3</sup> (Smrkovec), and  
83  $a=13.620(1)$ ,  $c=5.903(1)$  Å,  $V=948.2(2)$  Å<sup>3</sup> (Jáchymov), are comparable with the data  
84 published for this mineral phase<sup>10,29</sup>.

85

86 The mineral samples were analysed by electron microprobe (Cameca SX100, WD  
87 mode) for chemical composition. The results (Smrkovec - mean of 3 point analysis) are CaO  
88 0.85, FeO 0.11, PbO 3.06, CuO 41.76, Al<sub>2</sub>O<sub>3</sub> 0.03, Bi<sub>2</sub>O<sub>3</sub> 16.24, SiO<sub>2</sub> 0.83, As<sub>2</sub>O<sub>5</sub> 26.65,  
89 P<sub>2</sub>O<sub>5</sub> 1.87, H<sub>2</sub>O (10.12), sum 102.13 wt. %, and empirical formula:

90  $(\text{Bi}_{0.77}\text{Ca}_{0.17}\text{Pb}_{0.15}\text{Fe}_{0.11})_{\Sigma 1.20}\text{Cu}_{5.79}[(\text{AsO}_4)_{2.17}(\text{AsO}_3\text{OH})_{0.39}(\text{PO}_4)_{0.29}(\text{SiO}_4)_{0.15}]_{\Sigma 3.00}(\text{OH})_{6.00} \cdot$

91  $3\text{H}_2\text{O}$ ; Jáchymov (mean of 3 point analyses): CaO 0.50, FeO 0.14, PbO 2.77, Cu 44.22,

92 Al<sub>2</sub>O<sub>3</sub> 0.14, Bi<sub>2</sub>O<sub>3</sub> 16.16, SiO<sub>2</sub> 1.04, As<sub>2</sub>O<sub>5</sub> 26.32, P<sub>2</sub>O<sub>5</sub> 1.99, H<sub>2</sub>O (10.01), sum 103.29 wt. %

93 resulting to empirical formula  $(\text{Bi}_{0.76}\text{Pb}_{0.14}\text{Ca}_{0.10}\text{Al}_{0.03}\text{Fe}_{0.02})_{\Sigma 1.05}\text{Cu}_{6.08}$

94  $[(\text{AsO}_4)_{2.34}(\text{AsO}_3\text{OH})_{0.16}(\text{PO}_4)_{0.31}(\text{SiO}_4)_{0.19}]_{\Sigma 3.00}(\text{OH})_{6.00} \cdot 3\text{H}_2\text{O}$ . The basis of recalculating is

95  $(\text{P}+\text{As}+\text{Si}) = 3.00$  apfu; water contents were calculated on the basis of theoretical content

96  $\text{H}_2\text{O} = 3$  pfu and charge balance.

97

### 98 **Raman spectroscopy**

99

100 The crystals of mixite were placed and oriented on a polished metal surface on the  
101 stage of an Olympus BHSM microscope, which is equipped with 10x and 50x objectives. The

102 microscope is part of a Renishaw 1000 Raman microscope system, which also includes a  
103 monochromator, a notch filter system and a CCD detector. The Raman spectra were excited  
104 by a He-Ne laser producing highly polarized light at 633 nm and collected at a nominal  
105 resolution of  $2\text{ cm}^{-1}$  and a precision of  $\pm 1\text{ cm}^{-1}$  in the range between 100 and  $4000\text{ cm}^{-1}$ .  
106 Repeated acquisition on the crystals using the highest magnification (50x) were accumulated  
107 to improve the signal to noise ratio. Spectra were calibrated using the  $520.5\text{ cm}^{-1}$  line of a  
108 silicon wafer. The laser power was measured as 0.1 watts. Previous studies by the authors  
109 provide more details of the experimental technique. Further details have been published<sup>30-33</sup>.  
110

### 111 **Infrared spectroscopy**

112  
113 Infrared spectra of both mixite samples were recorded by micro diffuse reflectance  
114 method (DRIFTS) on a Nicolet Magna 760 FTIR spectrometer (range  $4000\text{-}600\text{ cm}^{-1}$ ,  
115 resolution  $4\text{ cm}^{-1}$ , 128 scans, 2 level zero-filtering, Happ-Genzel apodization), equipped with  
116 Spectra Tech InspectIR micro FTIR accessory. Each sample of amount less than 0.050 mg  
117 was mixed without using pressure with KBr. Samples were immediately recorded together  
118 with the same KBr as a reference.

119  
120 Band component analyses for both Raman and infrared spectra were undertaken using  
121 the Jandel 'Peakfit' software package, which enabled the type of fitting function to be  
122 selected and allows specific parameters to be fixed or varied accordingly. Band fitting was  
123 done using a Lorentz- Gauss cross-product function with the minimum number of component  
124 bands used for the fitting process. The Lorentz- Gauss ratio was maintained at values greater  
125 than 0.7 and fitting was undertaken until reproducible results were obtained with squared  
126 regression coefficient of  $R^2$  greater than 0.995.

127

## 128 **RESULTS AND DISCUSSION**

129 According to Myneni *et al.*<sup>38,39</sup> and Nakamoto<sup>40</sup>,  $(\text{AsO}_4)^{3-}$  is a tetrahedral unit, which  
130 exhibits four fundamental vibrations: the  $\nu_1$  symmetric stretching vibration ( $A_1$ )  $818\text{ cm}^{-1}$ ,  
131 Raman active; the doubly degenerate  $\nu_2$  symmetric bending vibration (E)  $350\text{ cm}^{-1}$ , Raman  
132 active; the triply degenerate  $\nu_3$  antisymmetric stretching vibration ( $F_2$ )  $786\text{ cm}^{-1}$ , and the

133 triply degenerate  $\nu_4$  bending vibration ( $F_2$ )  $405\text{ cm}^{-1}$ , both infrared and Raman active.  
 134 Protonation, metal complexation, and/or adsorption on a mineral surface should cause change  
 135 in  $(\text{AsO}_4)^{3-}$  symmetry from  $T_d$  to lower symmetries, such as  $C_{3v}$ ,  $C_{2v}$ ,  $C_1$ . This is connected  
 136 with the splitting of degenerate vibrations of  $(\text{AsO}_4)^{3-}$  and the shifting of the As-OH  
 137 stretching vibrations to different wavenumbers. Such chemical interactions reduce  $(\text{AsO}_4)^{3-}$   
 138 tetrahedral symmetry, as mentioned above, to either  $C_{3v}/C_3$  (corner-sharing),  $C_{2v}/C_2$  (edge-  
 139 sharing, bidentate binuclear), or  $C_1/C_s$  (corner-sharing, edge-sharing, bidentate binuclear,  
 140 multidentate)<sup>38,39</sup>. In association with  $(\text{AsO}_4)^{3-}$  symmetry and coordination changes, the  $A_1$   
 141 band may shift to different wavenumbers and the doubly degenerate E and triply degenerate F  
 142 modes may give rise to several new  $A_1$ ,  $B_1$ , and/or E vibrations<sup>38,39</sup>. In the absence of  
 143 symmetry deviations,  $(\text{AsO}_3\text{OH})^{2-}$  in  $C_{3v}$  symmetry exhibit the  $\nu_s$  As-OH and  $\nu_{as}$  and  $\nu_s$  As-  
 144  $\text{O}_3$  vibrations together with corresponding the  $\delta$  As-OH in-plane bending vibration,  $\delta$  As-OH  
 145 out-of-plane bending vibration,  $\nu_s$  As- $\text{O}_3$  stretching vibration and  $\delta_{as}$  As- $\text{O}_3$  bending vibration  
 146<sup>36,37,41</sup>. Keller<sup>41</sup> assigned observed the following infrared bands in  $\text{Na}_2(\text{AsO}_3\text{OH})\cdot 7\text{H}_2\text{O}$   $450$   
 147 and  $360\text{ cm}^{-1}$  to the  $\delta_{as}$  ( $\nu_4$ )  $\text{AsO}_3$  bend (E),  $580\text{ cm}^{-1}$  to the  $\delta$  As-OH out-of-plane bend,  $715$   
 148  $\text{cm}^{-1}$  to the  $\nu$  As-OH stretch ( $A_1$ ),  $830\text{ cm}^{-1}$  to the  $\nu_{as}$   $\text{AsO}_3$  stretch (E), and  $1165\text{ cm}^{-1}$  to the  $\delta$   
 149 As-OH in plane bend. In the Raman spectrum of  $\text{Na}_2(\text{AsO}_3\text{OH})\cdot 7\text{H}_2\text{O}$ , Vansant *et al.*<sup>36</sup>  
 150 attributed observed Raman bands to the following vibrations  $55$ ,  $94$ ,  $116$  and  $155\text{ cm}^{-1}$  to  
 151 lattice modes,  $210\text{ cm}^{-1}$  to  $\nu$  (OH...O) stretch,  $315\text{ cm}^{-1}$  to  $\text{AsO}_3$  rocking,  $338\text{ cm}^{-1}$  to the  $\delta_s$   
 152  $\text{AsO}_3$  bend,  $381\text{ cm}^{-1}$  to the  $\delta_{as}$   $\text{AsO}_3$  bend,  $737\text{ cm}^{-1}$  to the  $\nu_s$  As-OH stretch ( $A_1$ ),  $866\text{ cm}^{-1}$  to  
 153 the  $\nu_{as}$  stretch (E). Because of relatively high content of  $\text{P}^{5+}$  ( $\sim 0.3$  apfu), also bands related to  
 154 the  $(\text{PO}_4)^{3-}$  and  $(\text{PO}_3\text{OH})^{2-}$  vibrations are expected to be observed in the Raman and infrared  
 155 spectra ( $(\text{PO}_4)^{3-}$ :  $\delta_s$  ( $\nu_2$ )  $410\text{-}490\text{ cm}^{-1}$ ,  $\delta_{as}$  ( $\nu_4$ )  $510\text{-}670\text{ cm}^{-1}$ ,  $\nu_1$   $930\text{-}990\text{ cm}^{-1}$ ,  $\nu_3$   $975\text{-}1140$   
 156  $\text{cm}^{-1}$ ;  $(\text{PO}_3\text{OH})^{2-}$ :  $\delta$  ( $\text{O}_3\text{PO}$ )  $350\text{-}580\text{ cm}^{-1}$ ,  $\gamma$  POH  $700\text{-}900\text{ cm}^{-1}$ ,  $\nu$  POH  $860\text{-}915\text{ cm}^{-1}$ ,  $\nu_s$   $\text{PO}_3$   
 157  $940\text{-}1010\text{ cm}^{-1}$ ,  $\nu_{as}$   $1040\text{-}1170\text{ cm}^{-1}$ ,  $\delta$  POH  $1210\text{-}1400\text{ cm}^{-1}$ , and combination bands at  $1400\text{-}$   
 158  $1750\text{ cm}^{-1}$ ), if they are Raman and/or infrared active<sup>42</sup>.

159  
 160 Mixite is the mineral with a general formula  $\text{BiCu}_6(\text{AsO}_4)_3(\text{OH})_6\cdot 3\text{H}_2\text{O}$  and as such  
 161 will have three different vibrating units which will contribute to the overall spectral profile:  
 162 (a) namely the OH units (b) the water molecules and (c) the arsenate  $(\text{AsO}_4)^{3-}$  groups – a part  
 163 of them, however, may be substituted by  $(\text{AsO}_3\text{OH})^{2-}$  groups because of necessary charge  
 164 balance. The first two vibrating species will contribute to the high wavenumber region whilst  
 165 the  $(\text{AsO}_4)^{3-}$  and  $(\text{AsO}_3\text{OH})^{2-}$  units will show Raman bands below  $1000\text{ cm}^{-1}$ <sup>34</sup>. Vibrational

166 spectroscopy has been used to study the coordination chemistry of  $(\text{AsO}_4)^{3-}$  ions for some  
167 considerable time<sup>34-39</sup>. Vibrational spectroscopic studies have shown that the symmetry of  
168 the  $(\text{AsO}_4)^{3-}$  polyhedron are strongly distorted and the  $(\text{AsO}_4)^{3-}$  vibrations are strongly  
169 influenced by protonation, cation presence and water coordination<sup>36-39</sup>. Of all the tetrahedral  
170 oxyanions, the positions of the arsenate vibrations occur at lower wavenumbers than any of  
171 the other naturally occurring mineral oxyanions. There are one symmetrically distinct  
172  $\text{M}^{3+}/\text{M}^{2+}$  ( $\text{Bi}^{3+}/\text{Ca}^{2+}$ ), one symmetrically distinct  $\text{Cu}^{2+}$ , and one symmetrically distinct  $\text{As}^{5+}$  in  
173 the crystal structure of mixite<sup>10</sup>. Respecting the existence of only one As site and a disorder  
174 character of substitution  $(\text{OH})^- \Leftrightarrow \text{O}^{2-}$  at one oxygen position, mixite may be formulated as  
175  $(\text{M}^{3+}, \text{M}^{2+})\text{Cu}_6[(\text{As},\text{P})\text{O}_3(\text{O},\text{OH})]\cdot 3\text{H}_2\text{O}$ . No substantial differences in unit cell parameters are  
176 between the studied mixite samples. Mixite from Jáchymov slightly differs from the mixite  
177 from Smrkovec in the content of  $\text{P}^{5+}$  (0.31/0.29 apfu),  $\text{Si}^{4+}$  (0.19/0.15 apfu), and significantly  
178 in calculated  $(\text{AsO}_3\text{OH})^{2-}$  content (0.16/0.39 apfu).

179

180 The stretching vibrations of  $[(\text{As},\text{P})\text{O}_3(\text{O},\text{OH})]$  units in mixite from Smrkovec and  
181 Jáchymov in the 700 to 1200  $\text{cm}^{-1}$  region of the Raman spectra are shown in Fig. 1. The  
182 infrared spectra of both mineral samples are given in Fig. 2. The spectra of the two mixite  
183 samples are very similar as expected. An intense Raman band is observed at  $\sim 850 \text{ cm}^{-1}$  for  
184 mixite. This band is assigned to the  $\nu_1 (\text{AsO}_4)^{3-}$  symmetric stretching vibration. It corresponds  
185 to an infrared band at 848  $\text{cm}^{-1}$  (S) and 844  $\text{cm}^{-1}$  (J). Raman and infrared bands of the  $\nu$   
186  $(\text{AsO}_3)$  symmetric and antisymmetric stretching vibrations may overlap the  $\nu_1 (\text{AsO}_4)^{3-}$  band.  
187 Other Raman bands (855 and 805  $\text{cm}^{-1}$  (S), 881, 837 and 806  $\text{cm}^{-1}$  (J)) and infrared bands  
188 (814 and 797  $\text{cm}^{-1}$  (S) and 807 and 799  $\text{cm}^{-1}$  (J)) are assigned to the split  $\nu_3 (\text{AsO}_4)^{3-}$   
189 antisymmetric stretching vibrations,  $\nu_{\text{as}} (\text{AsO}_3)$  stretching vibrations and those close to 725  
190 and 700  $\text{cm}^{-1}$  to the  $\nu$  As-OH stretching vibrations of the  $(\text{AsO}_3\text{OH})^{2-}$  units. Raman bands at  
191 955  $\text{cm}^{-1}$  (S) and 991  $\text{cm}^{-1}$  (J) and infrared bands at 1012 and 970  $\text{cm}^{-1}$  (S) and 1173, 1110,  
192 1089, 1057 and 997  $\text{cm}^{-1}$  (J) are attributed to the  $\nu_3$  and  $\nu_1 (\text{PO}_4)^{3-}$  stretching vibrations. Some  
193 of these bands, however, may be connected with the  $\delta$  As-OH in-plane bending vibrations  
194 and  $\delta$  P-OH in-plane bending vibrations and  $\nu_{\text{as}} (\text{PO}_3)$  stretching vibrations of  $(\text{AsO}_3\text{OH})^{2-}$   
195 and  $(\text{PO}_3\text{OH})^{2-}$  units<sup>36-39,41,42</sup>. Infrared bands at 657  $\text{cm}^{-1}$  (S) and 607  $\text{cm}^{-1}$  (J) may be  
196 probably related to the libration mode of water molecules.

197

198 A number of Raman bands are observed in the 350 to 550  $\text{cm}^{-1}$  region (Fig. 3). Bands  
199 at 553, 529 and 494  $\text{cm}^{-1}$  (S) and 554, 531 and 500  $\text{cm}^{-1}$  (J) are assigned to the  $\delta_{\text{as}}$  ( $\nu_4$ ) triply  
200 degenerate  $(\text{PO}_4)^{3-}$  bending vibrations,  $\delta_{\text{as}}$  doubly degenerate  $(\text{PO}_3)$  bending vibration, and  
201  $\delta_{\text{As-OH}}$  out-of-plane bending vibration<sup>41</sup>. Bands at 472 and 460  $\text{cm}^{-1}$  (S) and 472 and 421  
202  $\text{cm}^{-1}$  (J) may be assigned to the  $\delta_{\text{as}}$  ( $\nu_4$ ) triply degenerated  $(\text{AsO}_4)^{3-}$  bending vibration,  $\delta_{\text{as}}$   
203  $(\text{AsO}_3)$  bending vibration and  $\delta_{\text{as}}$  ( $\nu_2$ )  $(\text{AsO}_4)^{3-}$  doubly degenerate bending vibration. Bands at  
204 390 and 311  $\text{cm}^{-1}$  (S) and 390 and 317  $\text{cm}^{-1}$  (J) are assigned to the  $\delta_{\text{s}}$  ( $\nu_2$ ) doubly degenerate  
205  $(\text{AsO}_4)^{3-}$  bending vibration and  $\delta$  doubly degenerate  $(\text{AsO}_3)$  bending vibration<sup>36,37,41</sup>. Raman  
206 bands in the region from 284 to 105  $\text{cm}^{-1}$  (S) and 282 to 106  $\text{cm}^{-1}$  (J) may be related to cation-  
207 oxygen vibrations and lattice vibrations.

208  
209 The Raman spectra of the  $\nu$  OH stretching region are shown in Fig. 4 and the infrared  
210 spectra are given in Fig. 5. Sharp Raman bands at 3470  $\text{cm}^{-1}$  (S) and 3451  $\text{cm}^{-1}$  (J) together  
211 with sharp infrared bands at 3483  $\text{cm}^{-1}$  (S) and 3483  $\text{cm}^{-1}$  (J) are assigned to the weakly  
212 hydrogen bonded hydroxyl ions. Corresponding O-H...O hydrogen bond lengths are ( $\text{\AA}/\text{cm}^{-1}$ )  
213 2.87/3470 and 2.88/3483(S) and 2.85/3451 and 2.88/3483 (J)<sup>43</sup>. Such hydrogen bonds may  
214 be understood as weak, because they are over 2.70  $\text{\AA}$ <sup>43-45</sup>. Raman bands at 3361  $\text{cm}^{-1}$  (S) and  
215 3392  $\text{cm}^{-1}$  (J) and infrared bands at 3381 and 3243  $\text{cm}^{-1}$  (S) and 3372, 3222 and 2977  $\text{cm}^{-1}$  (J)  
216 are assigned to the weakly hydrogen bonded water molecules ( $\text{\AA}/\text{cm}^{-1}$ ) 2.79/3392, 2.79/3381  
217 and 2.73/3243  $\text{cm}^{-1}$  (S), and 2.78/3361, 2.79/3372, 2.72/3222  $\text{cm}^{-1}$  (J). According to Beran  
218 and Libowitzky<sup>43-45</sup>, these bonds are over 2.70  $\text{\AA}$  and therefore may be characterized as weak  
219 hydrogen bonds. Very weak infrared shoulders at 3554  $\text{cm}^{-1}$  (S) and 3554 and 2977  $\text{cm}^{-1}$  are  
220 not discussed. No Raman bands were observed in the region of bending vibrations of water  
221 molecules, however, infrared bands at 1624  $\text{cm}^{-1}$  (S) and 1631  $\text{cm}^{-1}$  (J) are assigned to the  $\delta$   
222 ( $\nu_2$ ) bending vibrations of water molecules. Raman bands at 1588 and 1513  $\text{cm}^{-1}$  (S) and  
223 1594 and 1511  $\text{cm}^{-1}$  (J) are characterized as combination bands<sup>42</sup>.

224

## 225 CONCLUSIONS

226

227 (1) Raman and infrared spectra of two mixite samples from Czech localities, containing  
228  $\sim 0.30 \text{ P}^{5+}$  apfu, were studied.

229 (2) The spectra of both mineral samples are practically very similar, some differences  
230 may be inferred in the organization of their hydrogen bonding network. Some



231 differences in band positions and intensities may be caused by different ratios of  
232  $(\text{AsO}_4)^{3-}$ ,  $(\text{AsO}_3\text{OH})^{2-}$ ,  $(\text{PO}_4)^{3-}$  and  $(\text{PO}_3\text{OH})^{2-}$  in the structure of studied mixite  
233 samples.

234 (3) Observed Raman and infrared bands were assigned to the stretching and bending  
235 vibrations of  $(\text{AsO}_4)^{3-}$ ,  $(\text{AsO}_3\text{OH})^{2-}$ ,  $(\text{PO}_4)^{3-}$  and  $(\text{PO}_3\text{OH})^{2-}$  units, hydroxyl ions and  
236 water molecules.

237 (4) O-H...O hydrogen bond lengths were inferred from both Raman and infrared  $\nu$  OH  
238 stretching vibrations. Hydrogen bond lengths are over 2.70 Å and may be therefore  
239 characterised as weak.

240

### 241 **Acknowledgements**

242

243 The financial and infrastructure support of the Queensland University of Technology  
244 Inorganic Materials Research Program of the School of Physical and Chemical Sciences is  
245 gratefully acknowledged. The Australian Research Council (ARC) is thanked for funding the  
246 Raman and infrared spectrometers. This work was financially supported by Ministry of  
247 Culture of the Czech Republic (DE07P04OMG004) to Jiří Sejkora and Jakub Plášil.

248

249

250

251

252

253

254

255

256

257

258

259 **REFERENCES**

- 260 1. Sejkora J, Řídkošil T, Šrein V *Neues Jahr. Min.* **1999**, *175*, 105-124.
- 261 2. Walenta K, Theye T *Aufschluss* **2004**, *55*, 17-23.
- 262 3. Walenta K, Theye T *Neues Jahr. Min.* **2005**, *181*, 219-222.
- 263 4. Sejkora J, Novotný P, Novák M, Šrein V, Berlepsch P *Can. Min.* **2005**, *43*, 1393-  
264 1400.
- 265 5. Walenta K *Erzgräber* **2003**, *17*, 46-51.
- 266 6. Olmi F, Sabelli C, Trosti Ferroni R *Neues Jahr. Min.* **1991**, 487-499.
- 267 7. Sejkora J, Šrein V *Zprávy o geologických výzkumech v roce 1995*, **1996**, 153-155.
- 268 8. Dietrich JE, Orliac M, Permingeat F *Bull. Soc. Franc. Min. Crist.* **1969**, *92*, 420-34.
- 269 9. Aruga A, Nakai I *Acta Cryst.* **1985**, *C41*, 161-3.
- 270 10. Mereiter K, Preisinger A *Öst. Akad. Wissen., math.-naturwiss. Kl.* **1986**, *123*, 79-81.
- 271 11. Zemann J *Mitteilungen der Österreichischen Mineralogischen Gesellschaft* **1991**, *136*,  
272 21-34
- 273 12. Miletich R, Zemann J *Aufschluss* **1993**, *44*, 17-21.
- 274 13. Miletich R, Zemann J, Nowak M *Phys. Chem. Min.* **1997**, *24*, 411-422.
- 275 14. Schrauf A *Zeit. Kryst.* **1880**, *4*, 277-281.
- 276 15. Frost RL, Weier M, Martens W, Duong L *Min. Mag.* **2005**, *69*, 169-177.
- 277 16. Frost RL, Weier M, Martens W *Spectrochim. Act.* **2006**, *A63*, 60-65
- 278 17. Frost RL, Mckinnon AR, Williams PA, Erickson KL, Weier ML, Leverett P *Neues*  
279 *Jahr. Min.* **2005**, *181*, 11-19.
- 280 18. Frost RL, Erickson KL, Weier ML, McKinnon AR, Williams PA, Leverett P *J.*  
281 *Raman Spectrosc.* **2004**, *35*, 961-966.
- 282 19. Frost RL, Weier M, Martens WN *Spectrochim. Act.* **2006**, *63*, 685-689.
- 283 20. Frost RL, Čejka J, Ayoko GA, Dickfos MJ *J. Raman Spectrosc.* **2008**, *39*, 374-379.
- 284 21. Frost RL, Čejka J, Dickfos MJ *J. Raman Spectrosc.* **2008**, *39*, 779-785.
- 285 22. Frost RL, Čejka J, Keeffe EC, Dickfos MJ *J. Raman Spectrosc.* **2008**, *39*, 1413-1418
- 286 23. Frost RL, Dickfos MJ, Čejka J *J. Raman Spectrosc.* **2008**, *39*, 1158-1161.
- 287 24. Frost RL, Dickfos MJ, Čejka J *J. Raman Spectrosc.* **2008**, *39*, 582-586.
- 288 25. Frost RL, Dickfos MJ, Reddy BJ *J. Raman Spectrosc.* **2008**, *39*, 1250-1256.
- 289 26. Frost RL, Hales MC, Wain DL *J. Raman Spectrosc.* **2008**, *39*, 108-114.
- 290 27. Frost RL, Keeffe EC *J. Raman Spectrosc.* **2008**, *39*, 1408-1412.
- 291 28. Sejkora J, Gabašová A, Novotná M *Bulletin mineralogicko-petrologického oddělení*  
292 *Národního muzea v Praze* **1997**, *4-5*, 185-187

- 293 29. Plášil J, Sejkora J, Čejka J, Škoda R, Goliáš V *J. Geosc.* **2009**, *54*, 15-56.
- 294 30. Frost RL, Čejka J, Dickfos MJ *J. Raman Spectrosc.* **2009**, *40*, 38-41.
- 295 31. Frost RL, Keeffe EC *J. Raman Spectrosc.* **2009**, *40*, 42-45.
- 296 32. Frost RL, Keeffe EC *J. Raman Spectrosc.* **2009**, *40*, 133-136.
- 297 33. Frost RL, Keeffe EC *J. Raman Spectrosc.* **2009**, *40*, 128-132.
- 298 34. Ross SD *Inorganic Infrared and Raman Spectra (European Chemistry Series)*, **1972**.
- 299 35. Siebert H Z. *Anorg. u. allgem. Chem.* **1954**, *275*, 225-40.
- 300 36. Vansant FK, Van der Veken BJ *J. Mol. Struc.* **1973**, *15*, 439-44.
- 301 37. Vansant FK, Van der Veken BJ, Desseyen HO *J. Mol. Struc.* **1973**,
- 302 *15*, 425-37.
- 303 38. Myneni SCB, Traina SJ, Waychunas GA, Logan TJ *Geochim. Cosmochim. Acta* **1998**, *62*, 3499-3514.
- 304
- 305 39. Myneni SCB, Traina SJ, Waychunas GA, Logan TJ *Geochim. Cosmochim. Acta* **1998**,
- 306 *62*, 3285-3300.
- 307 40. Nakamoto K *Infrared and Raman spectra of inorganic and coordination compounds*.
- 308 J. Wiley and Sons, New York 1986.
- 309 41. Keller P *Neues Jb. Miner. Mh.* **1971**, 491-510.
- 310 42. Pechkovskii VV, Melnikova PY, Dzyuba ED, Baranikova TI, Nikanovich MV, *Atlas*
- 311 *of infrared spectra of phosphates. Orthophosphates*. Nauka Moscow 1981. (in
- 312 Russian)
- 313 43. Libowitzky E, *Monatshefte für Chemie* **1999**, *130*, 1047-1059.
- 314 44. Beran A, Libowitzky E, *IR spectroscopy and hydrogen bonding in minerals*. In
- 315 *Microscopic Properties and Processes in Minerals* (K. Wright & R. Catlow, Eds.), p.
- 316 493-508, Kluwer Academic Publishers. Dordrecht, The Netherlands.
- 317 45. Libowitzky E, Beran A *EMU Notes in Mineralogy* **2006**, *6*, 227-279, Eötvös
- 318 University Press, Budapest.

319

320

321

322 **List of Figs.**

323

324 Fig. 1 Raman spectra of mixite from Smrkovec and Jáchymov in the 700 to 1200  $\text{cm}^{-1}$   
325 region.

326

327 Fig. 2 Infrared spectra of mixite from Smrkovec and Jáchymov in the 600 to 1200  $\text{cm}^{-1}$   
328 region.

329

330 Fig. 3 Raman spectra of mixite from Smrkovec and Jáchymov in the 100 to 700  $\text{cm}^{-1}$  region.

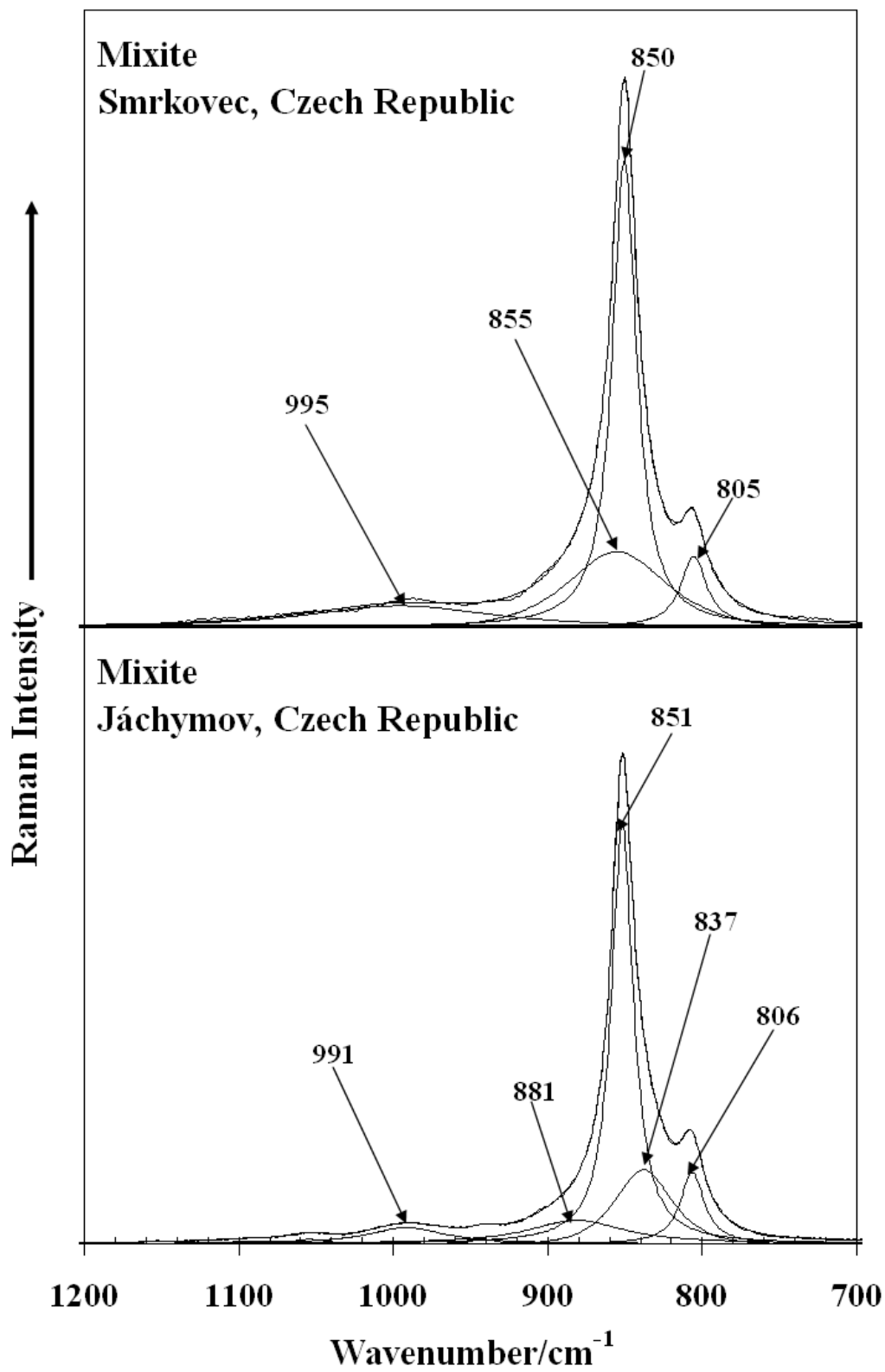
331

332 Fig. 4 Raman spectra of mixite from Smrkovec and Jáchymov in the 1200 to 3700  $\text{cm}^{-1}$   
333 region.

334

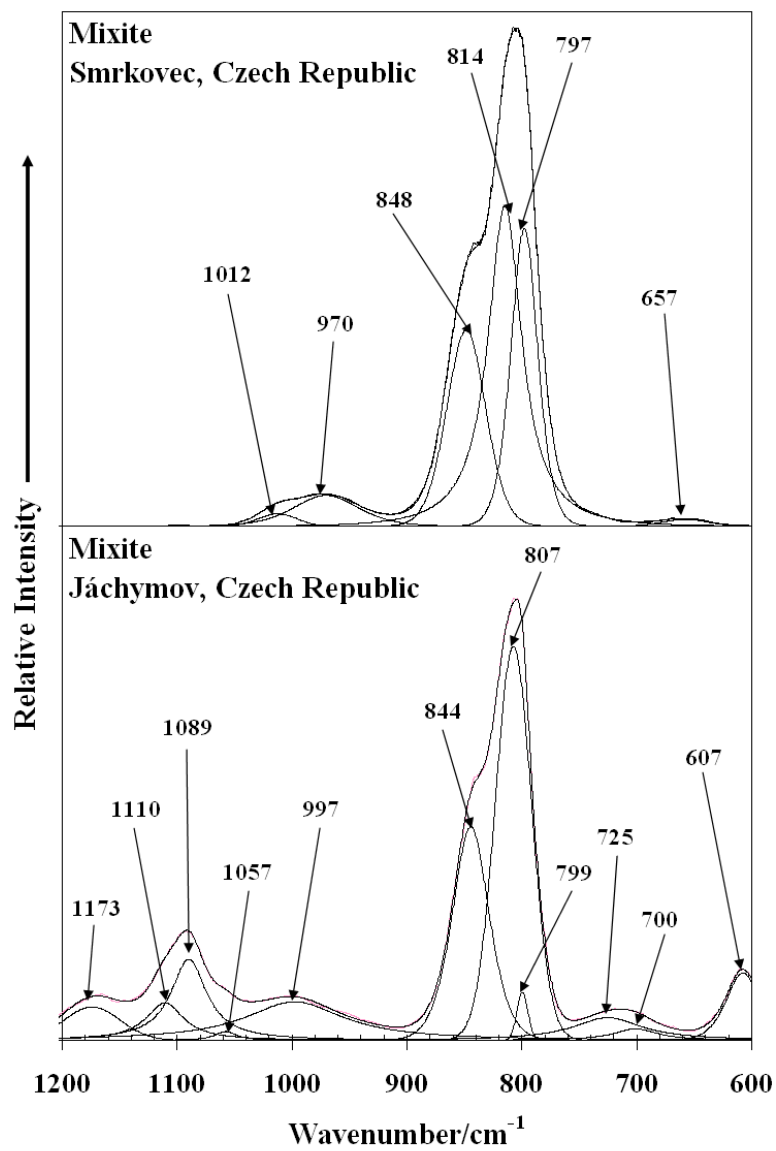
335 Fig. 5 Infrared spectra of mixite from Smrkovec and Jáchymov in the 1200 to 3800  $\text{cm}^{-1}$   
336 region.

337



338  
 339  
 340  
 341  
 342

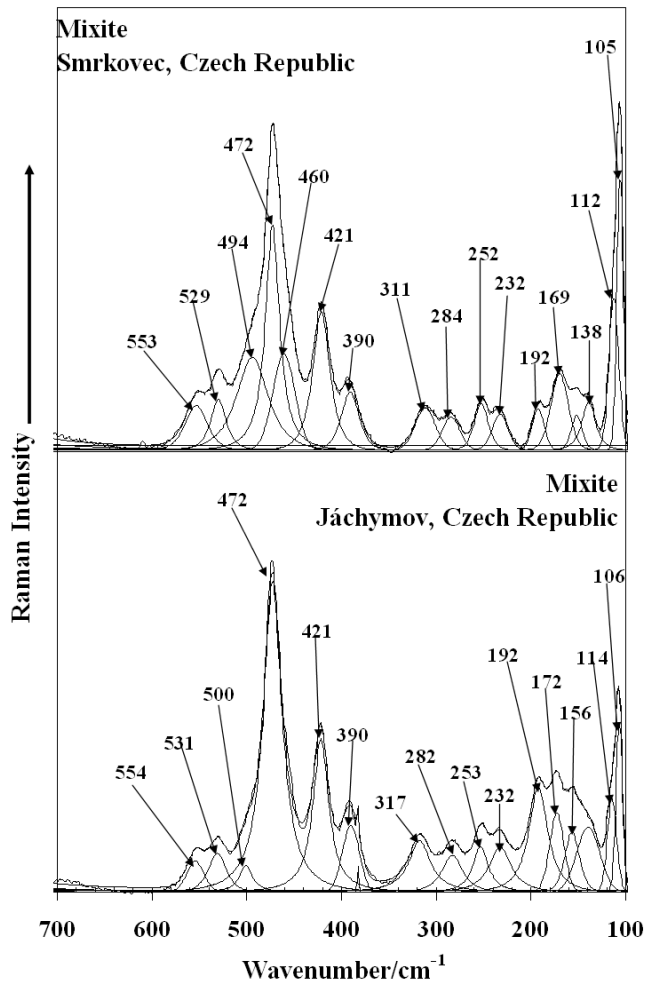
Fig. 1



343

344

345 **Fig. 2**



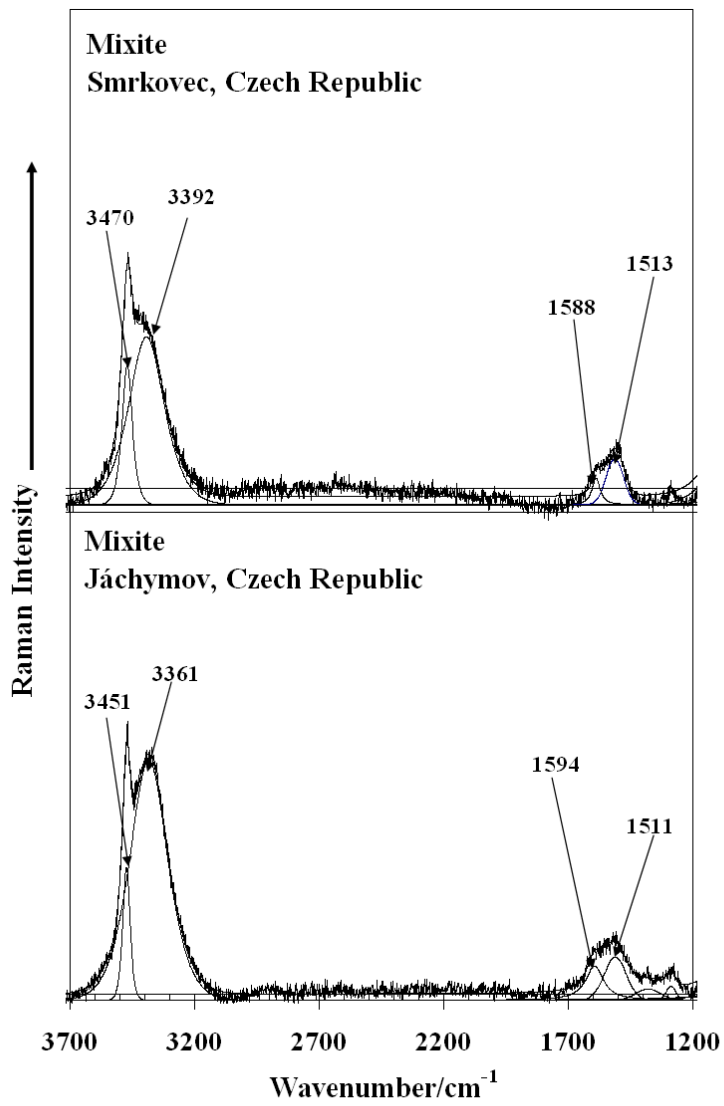
346

347

348 **Fig. 3**

349

350



351

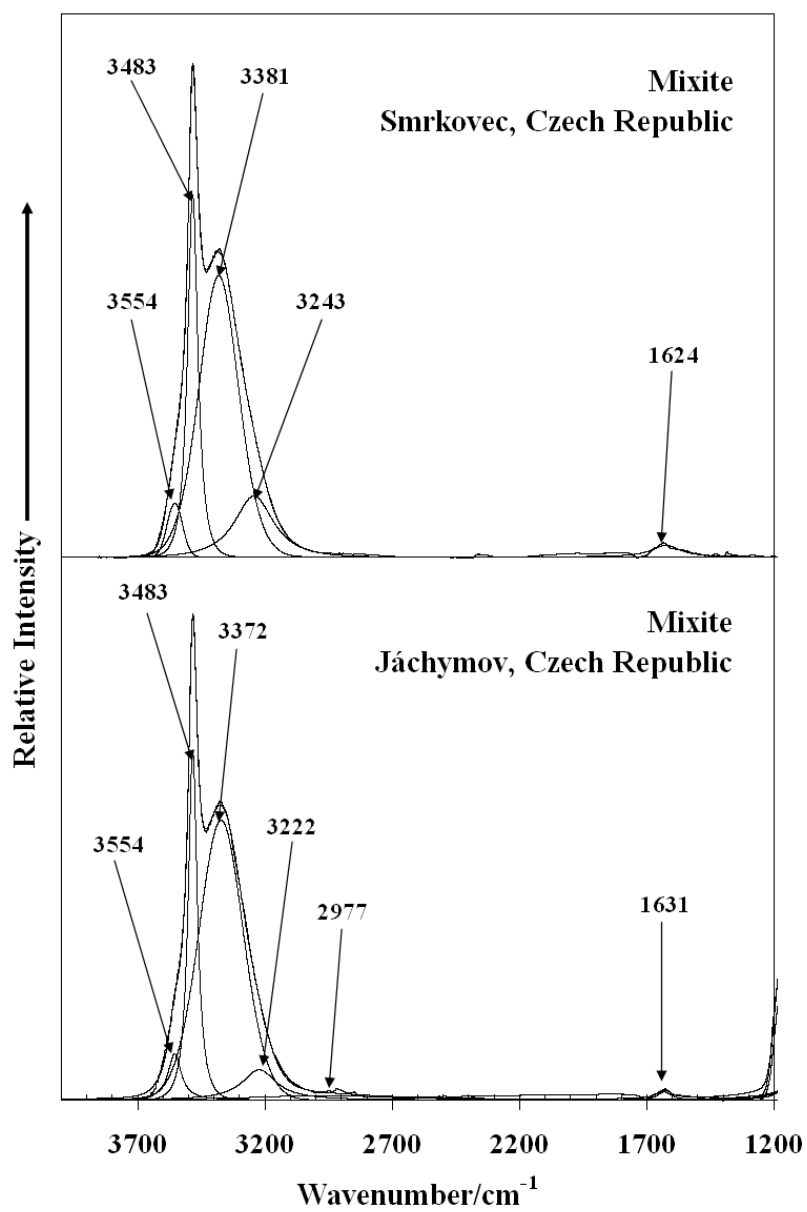
352

353 **Fig. 4**

354

355





356

357

358 **Fig. 5**

359